J. Fluid Mech. (1968), *vol.* 33, *part* 1, *pp.* 73–86
Printed in Great Britain

On the potential distribution resulting from flow across a magnetic field projecting from a plane wall

By ROGER C. BAKER
St John's College, Cambridge

(Received 4 April 1967 and in revised form 23 September 1967)

When a fluid of low conductivity flows parallel to a plane wall from behind which projects a magnetic field, an electric potential field is established throughout the fluid. In this paper the potential field is obtained explicitly in terms of the velocity field when the latter is unidirectional and depends only on the co-ordinate normal to the wall. Experiments with a variety of velocity profiles are described, and the agreement with the theory is satisfactory. The effect of slow variation of the profiles in the direction of the flow is considered, and is shown to be unimportant under the conditions of the experiments.

1. Introduction

It is sometimes desirable to measure the velocity of liquids in the neighbourhood of a plane wall, without introducing a probe into the fluid. One method which has been proposed for doing this is to measure the electric potentials generated at the wall surface, when the fluid flows through a magnetic field projected from behind the plane wall. Smith & Slepian (1917) patented a device of this kind for use as a ship's log, and Guelke & Schoute-Vanneck (1947) and Remenieras & Hermant (1954) have used a similar device for the measurement of ocean currents. Shercliff (1962) calls such a device an electromagnetic wall velometer. He has given solutions of the potential distribution for two limiting cases, first, of very thin boundary layers, when he considers the flow to be uniform, and, secondly, of very thick boundary layers, when he considers the flow to have a uniform shear profile with no slip at the wall.

In this paper the solution for an arbitrary velocity profile, which does not vary in the flow direction, is discussed. The effect on this solution of small variations of velocity in the flow direction, is considered. In conclusion some experiments are described which show that the solution gives good results for a variety of velocity profiles, even in cases where these have some variation in the flow direction.

2. Equations and boundary conditions

The usefulness of electromagnetic flow-measurement depends on being able to relate the potentials, which are induced by a fluid motion through a known magnetic field, to the velocity distribution. If the fluid is an electrolyte, an al-

ternating magnetic field is normally used to remove the problems connected with polarization. An alternating field of 50 c/s was used in the experiments described later in this paper; the working fluid was mains water.

The assumptions made in relating the various quantities are discussed by Shercliff (1962), and only those which are affected by the use of an alternating magnetic field are considered here.

The displacement current may be neglected provided that $\omega\epsilon/\sigma \ll 1$ (where ω is the frequency of the alternating magnetic field, ϵ is the permittivity and σ is the fluid conductivity). For $\omega = 100\pi$ rad/sec and $\sigma \simeq 10^{-2}$ mho/m, $\omega\epsilon/\sigma \simeq 2 \times 10^{-5}$.

Further simplification of the equations is obtained if the magnetic Reynolds number $\mu\sigma Va$ and the 'skin-depth' parameter $\mu\sigma\omega a^2$ are both small; (μ is the permeability of free space, V is a typical velocity and a is a typical length scale of the problem). With $a = 0{\cdot}1$ m, $V = 1$ m/sec and with the above values of σ and ω, $\mu\sigma Va \simeq 1{\cdot}3 \times 10^{-9}$ and $\mu\sigma\omega a^2 \simeq 4{\cdot}0 \times 10^{-6}$, and so the induced magnetic fields due both to the flow, and to the alternating applied field, may be neglected, and the equations for the magnetic field $\mathbf{B}$ may be written as

$$\mathbf{B} = \mathbf{B}_0 \sin \omega t, \quad \nabla \times \mathbf{B}_0 = 0 \quad \text{and} \quad \nabla . \mathbf{B}_0 = 0.$$

It follows immediately that $\nabla^2 \mathbf{B}_0 = 0$.

The quantity which is measured in flowmeters with an alternating magnetic field is the potential difference between the electrodes. The disadvantage of the alternating field is that in addition to the desired flow signals, which are in phase with the applied magnetic field, there may be unwanted signals whose phase is in quadrature with this field. These unwanted signals are caused by transformer action. This can be expressed by writing Ohm's law for each phase component:

$$\left.\begin{aligned} \mathbf{J}_1 \sin \omega t &= \sigma(\mathbf{E}_1 \sin \omega t + \mathbf{V} \times \mathbf{B}_0 \sin \omega t), \\ \mathbf{J}_2 \cos \omega t &= \sigma \mathbf{E}_2 \cos \omega t \end{aligned}\right\} \tag{2.1}$$

(where $\mathbf{J}$ is the current density and $\mathbf{E}$ is the electric field) and by writing the equations governing $\mathbf{E}$ in the same way

$$\left.\begin{aligned} \nabla \times \mathbf{E}_1 &= 0, \\ \nabla \times \mathbf{E}_2 &= -\omega \mathbf{B}_0. \end{aligned}\right\} \tag{2.2}$$

The component of $\mathbf{E}$, which is not in phase with the applied field and the flow signal, can be neglected if its value at the electrodes is small compared with the component of $\mathbf{E}$ in phase with the applied magnetic field, or alternatively if the amplifier is designed to reject signals in quadrature with the field. In practice, first, the effect of $\mathbf{E}_2$ on the electrode signal is reduced by careful positioning of the electrodes, and, secondly, the quadrature signals are rejected. The maximum value of the ratio of unwanted to wanted signals is $\omega a/V = 30$ for $\omega = 100\pi$ rad/sec, $a = 0{\cdot}1$ m and $V = 1$ m/sec. By taking advantage of symmetry in the field pattern the effect of this may be reduced to much less than unity at the electrodes, and the remainder rejected in the amplifier circuit.

It is thus necessary to consider only the components of quantities which are in

phase with the applied magnetic field. From (2.2), an electric potential U may be defined such that $\mathbf{E}_1 = -\nabla U$, and (2.1) then becomes

$$\mathbf{J}_1 = \sigma(-\nabla U + \mathbf{V} \times \mathbf{B}_0).$$

Since $\nabla . \mathbf{J}_1 = 0$, the divergence of this gives (with σ uniform)

$$\nabla^2 U = \mathbf{B}_0 . (\nabla \times \mathbf{V}), \tag{2.3}$$

and this is known as the flowmeter equation.

In practical designs the wall of the meter is non-conducting and the boundary condition there is obtained from Ohm's law by noting that the current perpendicular to the wall is zero, giving at the wall

$$(\nabla U)_\perp = (\mathbf{V} \times \mathbf{B}_0)_\perp, \tag{2.4}$$

(the subscript $_\perp$ indicating values in a direction perpendicular to the wall). For a non-slip condition on the velocity at the wall, this becomes simply

$$(\nabla U)_\perp = 0.$$

At boundaries 'at infinity' U is assumed to tend to zero.

3. Solution for the wall velometer

For velocity $(0, 0, V(x))$ (figure 1), and with $\mathbf{B}_0 = (B_x, B_y, B_z)$, (2.3) becomes

$$\nabla^2 U = -B_y \partial V(x)/\partial x, \tag{3.1}$$

while the boundary condition at the wall (2.4) becomes

$$\partial U/\partial x = -B_y(0, y, z)\, V(0). \tag{3.2}$$

The solution of (3.1) and (3.2) can be expressed in the form

$$U = \int_0^\infty V(\xi) B_y(2\xi + x, y, z) d\xi + \int_x^\infty V(\xi) B_y(2\xi - x, y, z) d\xi, \tag{3.3}$$

which may be derived by the use of the Fourier transforms of U and B_y with respect to the y-variable and standard algebraic manipulations (for details see Baker 1967*b*).† Here an alternative method of obtaining (3.3) is adopted, which gives some physical insight into the nature of the solution.

Since the relation between $V(x)$ and $U(x, y)$ is clearly linear, it will be sufficient to consider the effect of a single layer of moving fluid at $x = \xi$ (figure 1) which has velocity $V(\xi)$ and thickness $\delta\xi$ such that in the limit $\delta\xi \to 0$, $V(\xi)\delta\xi$ tends to a finite value. Suppose first that the remainder of space is filled with stationary fluid, and suppose that the field $\mathbf{B}$ emanates from singularities in the negative half space. The layer of moving fluid divides the space into two regions $x > \xi$ and $x < \xi$, (figure 1), and the potential is given by $\nabla^2 U = 0$ in each of these regions. Two boundary conditions are required to match U across the layer.

It may be observed that since $V(\xi)\delta\xi$ is finite as $\delta\xi$ tends to zero, so all quantities external to the layer will also be finite in the limit. Quantities within the layer will need more careful consideration. To obtain the relation between U

† Although the author obtained solutions of this type for the special cases of two-dimensional and axisymmetric fields, he is indebted to Mr M. K. Bevir for drawing his attention to the general applicability of the solution.

on each side of the layer, Ohm's law gives

$$\frac{J_x}{\sigma}\delta\xi = -(U_1 - U_2) - V(\xi)B_y(\xi, y, z)\delta\xi,$$

where the suffices 1 and 2 refer to conditions at $x = \xi+$ and $x = \xi-$ respectively.

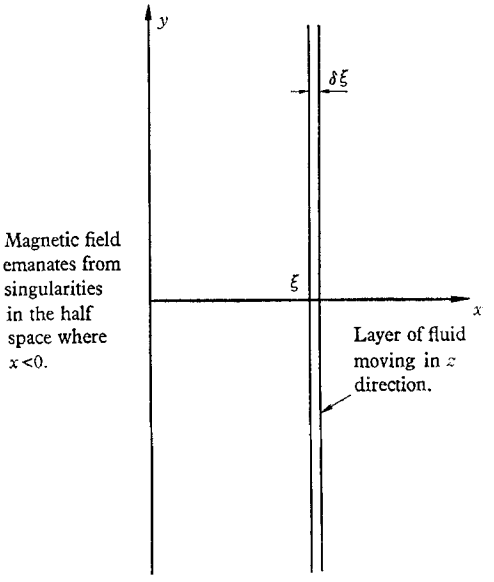

FIGURE 1. Co-ordinates used in §3.

In the limit $\delta\xi \to 0$, the term on the left vanishes since J_x is of the same order as the external current densities, and thus

$$U_1 - U_2 = -V(\xi)B_y(\xi, y, z)\delta\xi. \tag{3.4}$$

The significance of this condition is that the layer is acting as a voltage generator due to the presence of B_y. The Ohmic loss across the layer vanishes in the limit as the layer thickness becomes zero, while the e.m.f. generated by motion remains, causing currents to flow in the volume of stationary fluid.

The second condition is derived from the component of Ohm's law along the layer

$$\frac{J_y}{\sigma}\delta\xi = -\frac{\partial U}{\partial y}\delta\xi + V(\xi)B_x(\xi, y, z)\delta\xi.$$

In the limit $\delta\xi \to 0$, the final term remains finite. The potential gradient remains finite since it is a quantity which does not change in order of magnitude from values external to the layer. Thus $(\partial U/\partial y)\delta\xi \to 0$ as $\partial\xi \to 0$. Thus $\sigma^{-1}J_y\delta\xi$ will remain finite as $\delta\xi \to 0$ and the equation becomes

$$\frac{J_y}{\sigma}\delta\xi = V(\xi)B_x(\xi, y, z)\delta\xi.$$

Current continuity in the layer requires that

$$\left(\frac{\partial J_x}{\partial x} + \frac{\partial J_y}{\partial y} + \frac{\partial J_z}{\partial z}\right)\delta\xi = 0,$$

which becomes, in the limit $\delta\xi \to 0$,

$$J_{x_1} - J_{x_2} = -\frac{\partial J_y}{\partial y}\delta\xi,$$

since J_z is determined by the potential gradient only, which will be a finite quantity like the gradients external to the layer. Thus

$$J_{x_1} - J_{x_2} = -\sigma V(\xi)\frac{\partial B_x}{\partial y}(\xi, y, z)\delta\xi.$$

It is interesting to note that the layer is here acting as a current generator due to the presence of the x-component of $\mathbf{B}$, in which the net current leaving the layer is defined irrespective of the potential. But the current leaving the layer is also proportional to the potential gradient just outside the layer, so that, using $\nabla \times \mathbf{B} = 0$,

$$\left(\frac{\partial U}{\partial x}\right)_1 - \left(\frac{\partial U}{\partial x}\right)_2 = V(\xi)\frac{\partial B_y}{\partial x}(\xi, y, z)\delta\xi. \tag{3.5}$$

Since both U and B_y satisfy Laplace's equation outside the layer of moving fluid (apart from points where there are sources or sinks of magnetic field), the boundary conditions (3.4) and (3.5) suggest a direct relation between U and B_y at any point outside the layer, except that the gradient of potential must introduce a sign change. The condition can be satisfied by a potential distribution

$$U = \begin{cases} \alpha V(\xi) B_y(2\xi - x, y, z)\delta\xi & (x > \xi), \\ (\alpha + 1)\, V(\xi) B_y(2\xi - x, y, z)\delta\xi & (x < \xi), \end{cases}$$

where α is a constant to be determined later. The significance of this form of solution is that the potential on one side of the layer is directly proportional to the value of B_y at the symmetrical point on the other side of the layer. However B_y in the region $x < \xi$ has singularities and the solution above would require U to have singularities also. Since this is not so, α must be zero, leaving

$$U = \begin{cases} 0 & (x > \xi), \\ V(\xi) B_y(2\xi - x, y, z)\delta\xi & (x < \xi). \end{cases}$$

Insertion of a non-conducting wall at $x = 0$ will introduce the condition $\partial U/\partial x = 0$ there according to (3.2) (it is assumed that the strip of moving fluid is not adjacent to the wall). This boundary condition will be satisfied if an image of the layer is taken at $x = -\xi$, and the solution is modified accordingly. The solution then becomes

$$U = \begin{cases} V(\xi) B_y(2\xi + x, y, z)\delta\xi & (x > \xi), \\ V(\xi) B_y(2\xi - x, y, z)\delta\xi + V(\xi) B_y(2\xi + x, y, z)\delta\xi & (x < \xi). \end{cases}$$

For a general velocity profile $V(x)$, superposition of solutions of this form gives

$$U = \int_0^\infty V(\xi) B_y(2\xi + x, y, z)\, d\xi + \int_x^\infty V(\xi) B_y(2\xi - x, y, z)\, d\xi, \tag{3.3}$$

which is the result already quoted. Although this solution is derived for a non-slip velocity condition at the wall, it is also valid for a slip condition, as will be

shown. The application of a uniform velocity profile to (3.3) yields

$$U = V\int_x^\infty B_y(\xi, y, z)\,d\xi,$$

which is equivalent to the solution given by Shercliff (1962). Thus (3.3) is valid both for a non-slip velocity profile and for a uniform profile, and hence, by superposition, it is valid for a general profile with slip at the wall.

The potential at the wall is given by

$$U = \int_0^\infty V(\tfrac{1}{2}x)B_y(x, y, z)\,dx. \tag{3.6}$$

This is the special form of the solution which is applicable to the experiments discussed later.

The approximation that the profile is independent of the co-ordinate in the flow direction requires justification if this solution is to be applicable to the experimental work. In this a magnetic field symmetric about the x-axis was used. The effects of a varying velocity profile in the flow direction are apparent if the solution of (2.3) and (2.4) is expressed in terms of a Green's function. The potential drop between the points $(0, \pm a, 0)$ on the wall may then be expressed in the form

$$U(0,a,0) - U(0,-a,0) = -\frac{1}{2\pi}\iiint\left\{\frac{1}{[x^2+(y-a)^2+z^2]^{\frac{1}{2}}} - \frac{1}{[x^2+(y+a)^2+z^2]^{\frac{1}{2}}}\right\}\left\{\frac{\partial V_x}{\partial z} - \frac{\partial V_z}{\partial x}\right\}B_y\,dx\,dy\,dz \tag{3.7}$$

(where V_x and V_z are velocities in the x and z directions respectively). Expanding these by a Taylor series gives

$$\left.\begin{aligned} V_z(x,z) &= V(x,0) + z\frac{\partial V}{\partial z}(x,0) + \frac{z^2}{2}\frac{\partial^2 V}{\partial z^2}(x,0) + \ldots, \\ V_x(x,z) &= -\int_0^x \frac{\partial V}{\partial z}(x,0)\,dx - z\int_0^x \frac{\partial^2 V}{\partial z^2}(x,0)\,dx + \ldots. \end{aligned}\right\} \tag{3.8}$$

When the series are substituted in (3.7) $V(x,0)$ gives a contribution to the potential corresponding to the basic solution for a velocity distribution uniform in z. Terms with $\partial V(x,0)/\partial z$ form an integrand in (3.7) which is an odd function of z (assuming that B_y is an even function of z, as was the case in the experiments) and therefore the integral is zero. Terms with $\partial^2 V(x,0)/\partial z^2$ introduce a correction to the basic solution, the order of which is given by the product of typical values of $\partial^2 V(x,0)/\partial z^2$, B_y, and the cube of L the length scale (either for field or velocity variation, whichever is the less). Hence the correction will be of order $(L^2/V)(\partial^2 V(x,0)/\partial z^2)$ compared to the basic solution. This correction must be small for (3.6) to be useful.

4. Experiments on the wall velometer

A series of experiments were carried out to verify the theory of § 3. The device was mounted in one side of a water channel $35\frac{1}{2}$ cm wide. The depth of the channel was $11\frac{1}{2}$ cm and by a suitable arrangement of coils the magnetic field was designed to decay rapidly with depth so that the proximity of the opposite wall of the

channel could be neglected. The electrodes were arranged on the diameter perpendicular to the flow direction, and also on a circle concentric with the circular winding of the magnetic field coils.

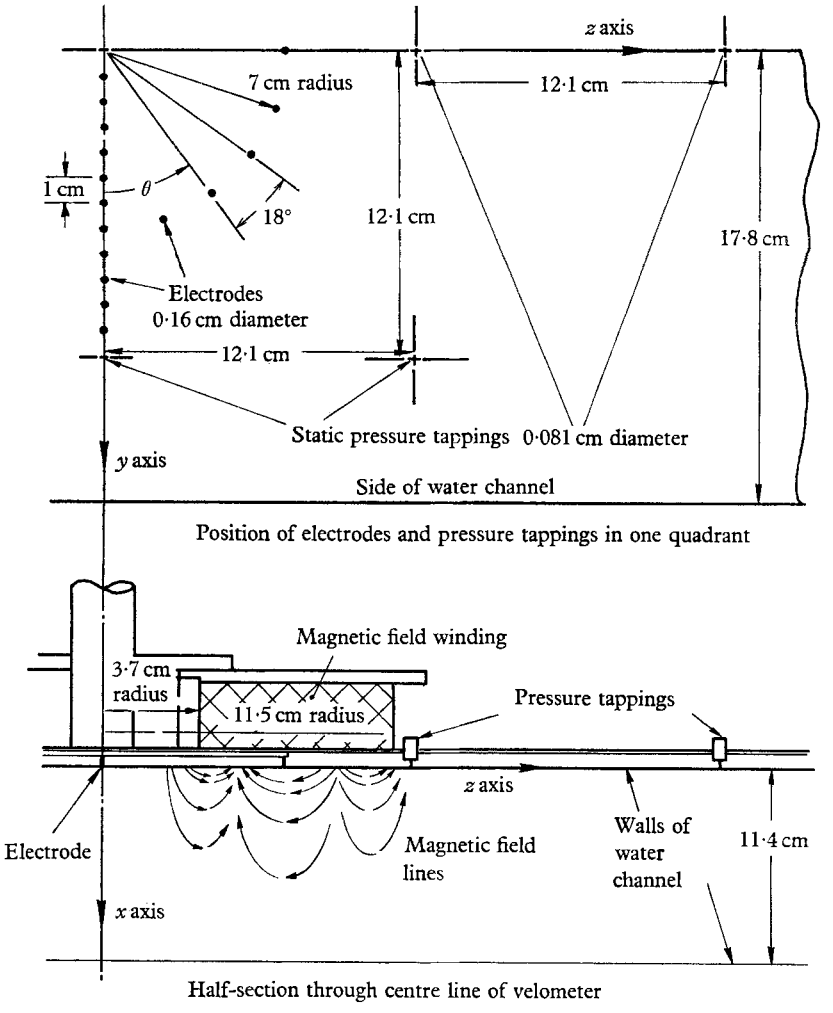

FIGURE 2. Velometer and channel details and co-ordinates (not to scale).

The potential difference between symmetrically placed electrodes was fed into an amplifier designed for electromagnetic flow-signal measurement. The principle of this amplifier has been described by Hutcheon & Harrison (1965). The output from the amplifier gave the ratio of the flow-signal to a reference signal which was proportional to the field excitation current. Thus values in this work are to a constant but arbitrary scale. The maximum potential difference shown in the results is of the order of one millivolt r.m.s.

The magnetic field was measured by means of a search coil which traversed through the field. This search coil had an area of 10·56 mm^2 and 30 turns. The

signal from this was passed through a 90° phase-changing circuit and then to the amplifier used in the measurement of the flow signals. This phase-changing circuit reduced the amplitude of the signals by one half. It was necessary since

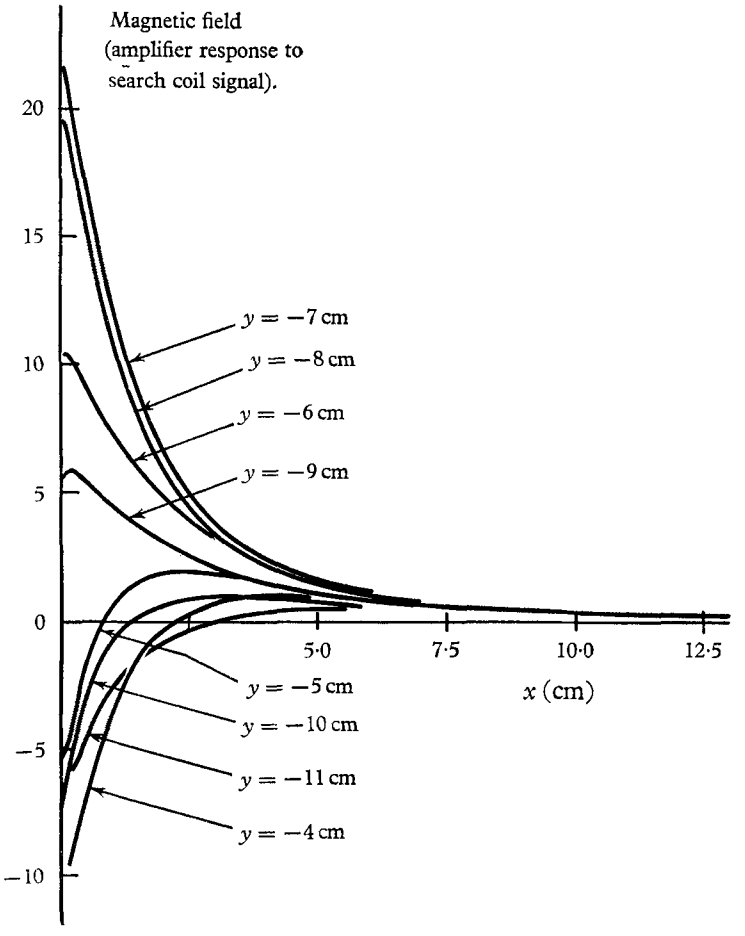

FIGURE 3. Variation of B_y with x at the electrode positions when $z = 0$ and y has the negative values shown.

the amplifier was designed to reject signals which were in quadrature with the reference signal. The variation of B_y with x at negative values of y for $z = 0$ is shown in figure 3. A slight variation from axisymmetry in the magnetic field was allowed for in calculation. The maximum field in this work was about 100 gauss r.m.s. These field measurements allowed a possible error of 3·5 %.

The velocity profile could be measured with a Pitot tube and static pressure tappings in the magnet wall. The experimental profiles obtained are shown in figures 4–6. Profile A was obtained by fitting a contraction upstream to give a submerged jet under the magnet. Profile B resulted from the flow passing over a step upstream. Profiles C and D were obtained with grids of rods fixed upstream to alter the velocity profile. Profiles E, F and G are turbulent boundary-layer

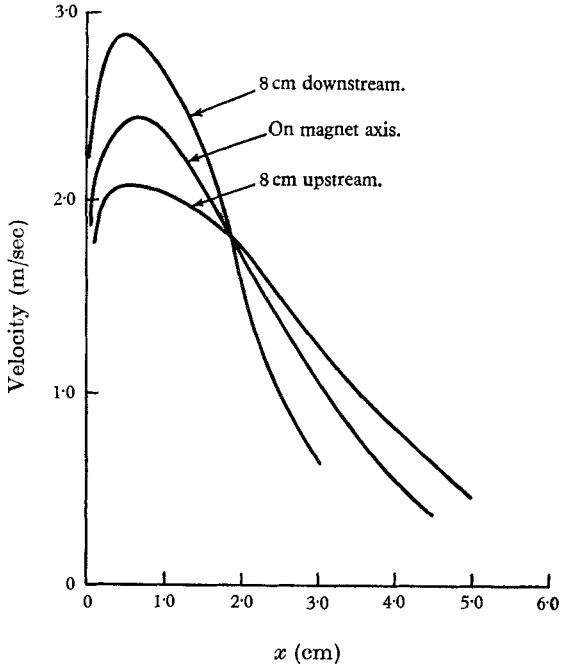

FIGURE 4. Velocity profiles for run A (submerged jet) for $y = 0$ and for three values of z.

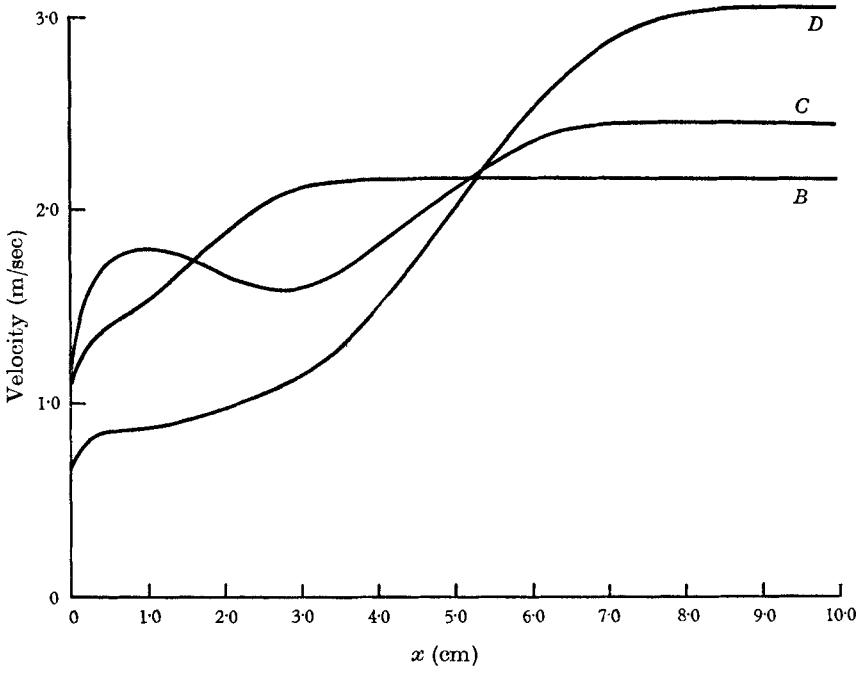

FIGURE 5. Velocity profiles for run B (step upstream) and for runs C and D (grids of rods upstream) for $y = z = 0$.

profiles formed by flow down the channel. The wide variation in these profiles was designed to check the validity of the solution of §3.

Due to the necessary proximity of the magnet to the water the static tappings were placed in the wall around the magnet, and thus the static pressure at points

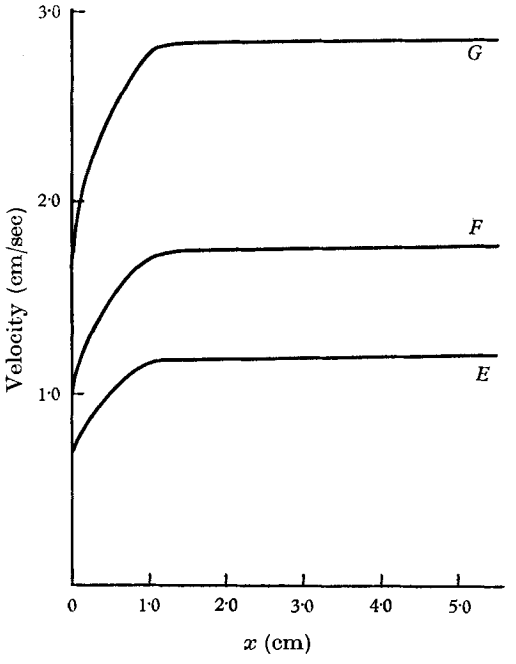

FIGURE 6. Velocity profiles for runs E, F and G (undistorted boundary layers) for $y = z = 0$.

under the magnet had to be estimated from values of static pressure at points around the magnet. This introduced a possible error of about 0·5 cm of water in all the runs except D when the uncertainty was about 5 cm of water.

In all runs the boundary-layer flow was turbulent, the Reynolds numbers based on boundary-layer thickness ranging from 10,000 to 250,000 approximately, and thus the Pitot tube gave a higher reading than it would have done for laminar flow. While no turbulence measurements were taken, the velometer gave an indication of the turbulence from the size of fluctuations of its output signal. In the case of run A this value was $\pm 6\%$ while for D it was $\pm 30\%$. However, in runs of boundary layer type it was much lower, being $\pm 2\%$ for E and $\pm 0{\cdot}4\%$ for F. Thus the Pitot tube readings will only be appreciably affected in run D.

The velocity profile was changing with z throughout these runs, and to assess this change it was measured for three values of z (figure 4 shows the changing profile for A, as an example). The correction which this variation will make to the basic solution, as discussed in §3, will be of order 5% for D, 1% for A, B and C and less than 0·5% for E, F and G. The non-uniformity of the flow across the stream was such as to allow a possible error of about 2% in some of the runs.

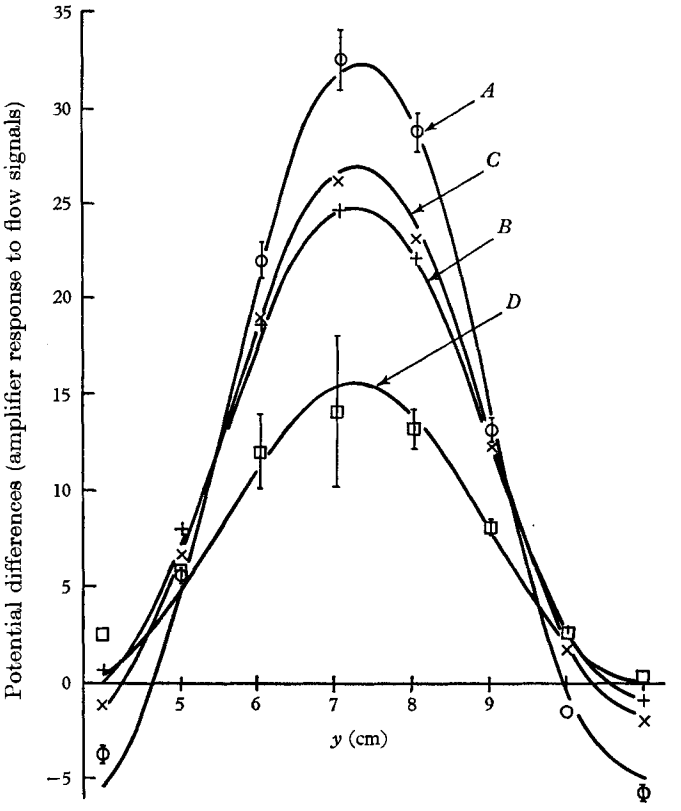

FIGURE 7. Potential differences between electrodes at $\pm y$ for $x = z = 0$ from theory (curves) and experiment (points).

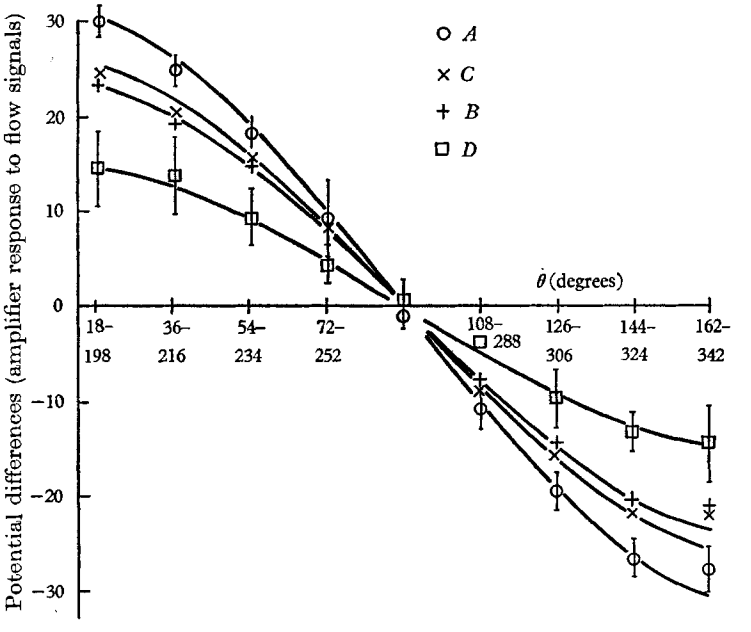

FIGURE 8. Potential differences between diametrically opposite electrodes at 7 cm radius from theory (curves) and experiment (points).

(The static pressures were so uncertain in run D that no useful estimate of the uniformity of the stream could be given.)

The distributions of B_y and velocity were used to determine the values to be expected for the potential distribution from (3.6). This was achieved with a

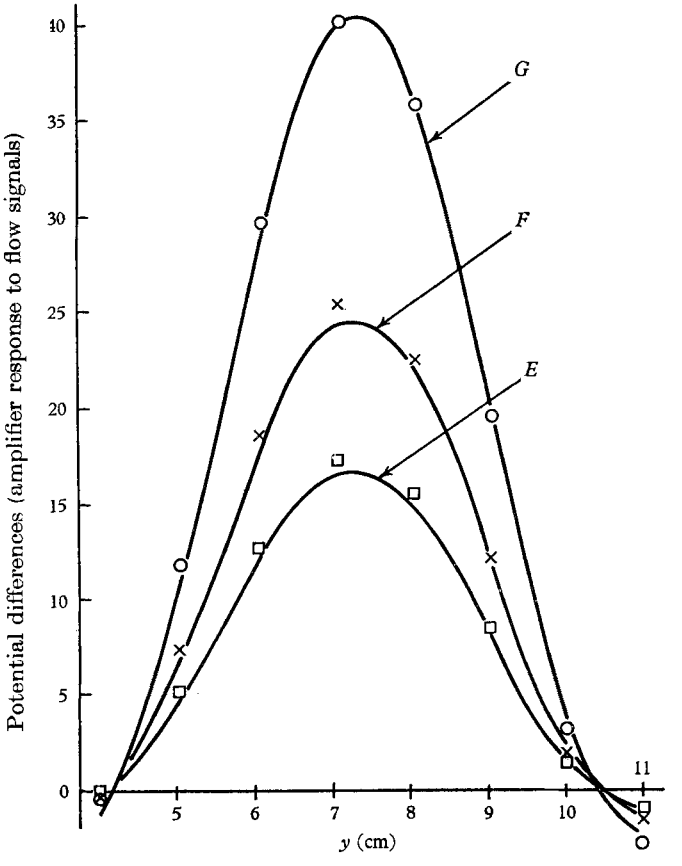

FIGURE 9. Potential differences between electrodes at $\pm y$ for $x = z = 0$ from theory (curves) and experiment (points).

computer program using Simpson's rule. A non-slip condition was assumed for the velocity at the wall. The resulting values are represented by the full curves in figures 7–10. Figures 7 and 9 compare these values with the experimentally obtained potential differences between symmetrically placed electrodes on the line $x = z = 0$ perpendicular to the flow for the velocity profiles of figures 4–6. Figures 8 and 10 do the same for diametrically opposite electrodes on the 7 cm radius circle concentric with the magnetic field excitation coil. The results obtained from the theory will be seen to agree with those obtained from the measurement of potential difference to within the limits of accuracy discussed above.

Full details of these experiments with further results are available (Baker 1967*b*).

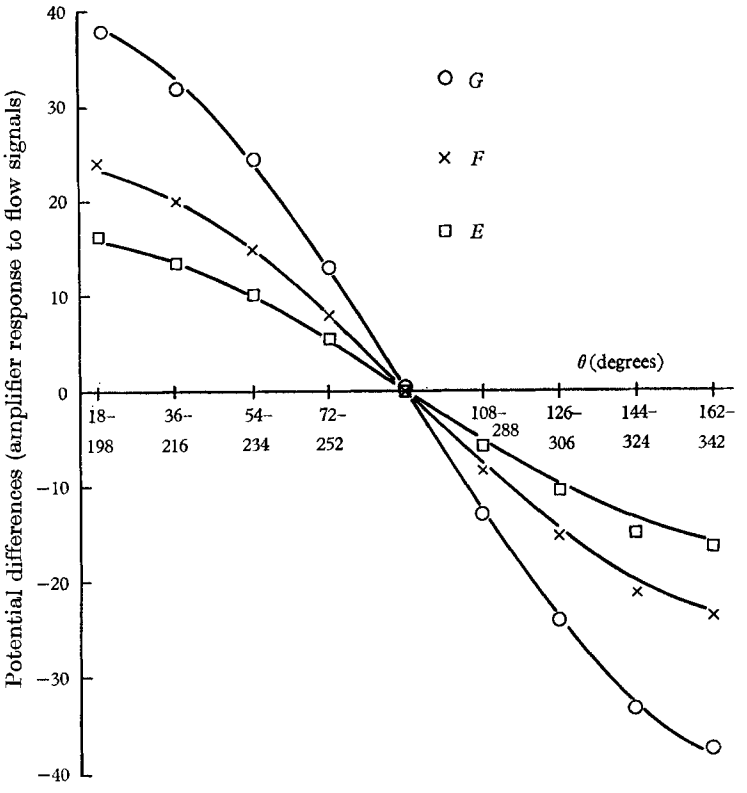

FIGURE 10. Potential differences between diametrically opposite electrodes at 7 cm radius from theory (curves) and experiment (points).

5. Conclusions

The solution obtained in §3 has been shown to give satisfactory results in practice even when the flow profile is changing to a small extent as it passes across the magnetic field. It would be useful if the device allowed the shape of the velocity profile to be obtained from the potential distribution at the wall. A method by which this might be achieved would be to equate the velocity profile in (3.6) to the sum of N velocity profiles with unknown coefficients. It would then theoretically be possible, by measuring the potential at N positions on the wall, to find the value of the unknown coefficients and hence a series representation of the velocity profile. This possibility was considered for various families of velocity profiles but due to the ill-conditioned nature of the resulting matrices and the experimental errors, no useful results were obtained.†

If some idea of the boundary-layer profile exists, then this device may be used to find some specific quantity. Of particular interest is the application to the measurement of ship's speed which was first suggested by Smith & Slepian (1917) and this possibility is being further considered (Baker 1967*a*). In this context, some idea of the boundary-layer shape is known and a field can be

† It is the opinion of the author that this approach is unlikely to succeed due to the problem of designing a field which will give a well-conditioned matrix.

designed to minimize the error due to changes in the boundary-layer shape and thickness.

The author would like to express gratitude to Prof. J. A. Shercliff for the initial encouragement to undertake this problem, to Dr. M. D. Cowley for most helpful advice on many aspects of this work and to Mr P. Austin for invaluable work in the construction of apparatus. The amplifier used in this work was kindly lent for this purpose by George Kent Limited and was one of their Veriflux Series 2 Converters.

REFERENCES

BAKER, R. C. 1967*a* British Patent Applications no. 6333/67 (9 February), and no. 8557/67 (22 February).

BAKER, R. C. 1967*b* Ph.D. Thesis. Cambridge University.

GUELKE, R. W. & SCHOUTE-VANNECK, C. A. 1947 *J. Inst. Elect. Engrs.* **94**, part 2, p. 71.

HUTCHEON, I. C. & HARRISON, D. N. 1965 *Instrument Practice*, **19**, 529.

REMENIERAS, G. & HERMANT, C. 1954 *La Houille Blanche*, **9**, 732.

SHERCLIFF, J. A. 1962 *The Theory of Electromagnetic Flow-Measurement.* Cambridge University Press.

SMITH, C. G. & SLEPIAN, J. 1917 U.S. Patent 1,249,530 (December).